

High-energy neutrino fluxes and flavor ratio in the Earth atmosphere

T.S. Sinegovskaya¹, A.D. Morozova², S.I. Sinegovsky³

¹ *Irkutsk State Railway University, 664074 Irkutsk, Russia*

² *Physics Faculty, Irkutsk State University, 664003 Irkutsk, Russia*

³ *Institute of Applied Physics, Irkutsk State University, 664003 Irkutsk, Russia*

High-energy neutrinos from decays of mesons, produced in collisions of cosmic-ray particles with air nuclei, form unavoidable background for detection of astrophysical neutrinos. More precise calculations of the high-energy neutrino spectrum are required since measurements in the IceCube experiment reach the intriguing energy range where a contribution of the prompt neutrinos and/or astrophysical ones should be uncovered. In this work, the calculation of muon and electron neutrino fluxes is performed for three hadronic models, QGSJET II, SIBYLL 2.1 and Kimel & Mokhov, taking into consideration the “knee” of the cosmic-ray spectrum. We calculate the atmospheric neutrino fluxes in the energy range 100 GeV – 10 PeV using parametrizations (models) of cosmic ray spectra over wide energy range by Zatsepin & Sokolskaya and Hillas & Gaisser as well as the polygonato model. In the computation, we employ the semianalytical approach to describe the hadron-nucleus cascade induced by cosmic rays in matter. The method allows to account the nonpower law energy spectrum of the primary cosmic rays, the violation of Feynman scaling, and the growth of the total inelastic cross sections for hadron-nucleus collisions with increasing energy. All calculations are compared with the atmospheric neutrino measurements by Frejus, AMANDA, IceCube and ANTARES. The prompt neutrino flux predictions obtained with the quark-gluon string model (QGSM) for the charm production by Kaidalov and Piskunova do not contradict to the measurements and upper limits on the astrophysical muon neutrino flux obtained with neutrino telescopes. The diffuse flux of astrophysical neutrinos related to the high-energy neutrino events in the IceCube experiment leads presumably to the flavor ratio decrease at the energy above 10 TeV. An extrapolation of the diffuse PeV neutrino flux to the energy range below 30 TeV shows the consistency of calculated neutrino flavor ratio and that of obtained from the IceCube data. The computation makes it clear that confirmation of astrophysical origin for high-energy neutrino events might be obtained from little progress in measurement of ν_e spectrum above 10 TeV, where the flavor ratio, responsive to changes in the electron neutrino flux, allows to reveal a small fraction from astrophysical sources.

PACS numbers: 13.85.Tp, 95.85.Ry, 95.55.Vj

I. INTRODUCTION

High-energy neutrinos produced in decays of pions, kaons, and charmed particles of the extensive air shower induced by cosmic rays passing through the Earth atmosphere, form an unavoidable background for the detection of astrophysical neutrinos. Search of extraterrestrial neutrino sources is the challenge to resolve which large-scale neutrino telescopes, NT200+ [1], IceCube [2–4], ANTARES [5, 6] are designed. The high-energy atmospheric neutrinos became accessible to the experimental studies only last years. By now, the energy spectrum of high-energy atmospheric muon neutrinos has been measured in three experiments: Frejus [7] at energies up to 1 TeV, AMANDA-II [8] in the energy range 1 – 100 TeV, IceCube40 [2] at 100 GeV – 400 TeV, and ANTARES at energies 100 GeV – 200 TeV [5]. Recently the IceCube presents also results for the electron neutrino spectrum measured in the energy range ~ 80 GeV – 6 TeV [9]. Thus one has a possibility to evaluate the neutrino flavor ratio using the IceCube measurements and to compare this one with predictions. Lately IceCube found the 28 high-energy neutrino events [10, 11] in energy range 30 TeV - 1.2 PeV, most of which are hardly consistent with events expected from the atmospheric neutrinos. The main reason to consider these events as produced by as-

trophysical neutrinos is the harder energy spectrum as compared to atmospheric neutrinos both the conventional and the prompt ones.

Increasing with the energy contribution of charmed particle decays to the neutrino flux becomes the source of the large uncertainty at energies above 100 TeV. Thus the comparison of the calculation for various hadron-interaction models with neutrino spectrum measurements is of much current interest, despite large statistical and systematic experimental errors in the high-energy region. Here we calculate atmospheric neutrino fluxes at energies $10^2 - 10^7$ GeV for zenith angles from 0° to 90° as well as the angle averaged spectrum with the use of high-energy hadronic interaction models QGSJET II-03 [12] and SIBYLL 2.1 [13]. These models are widely employed to simulate extensive air showers with the Monte Carlo method, and were also applied to compute the cosmic-ray hadron and muon fluxes [14, 15]. Besides, in this work computation, we employ also the known old hadronic model by Kimel & Mokhov (KM) [16] which was checked by comparison of the calculated atmospheric hadron and muon spectra with the experiment [14].

The calculation has been performed for three parametrizations of the experimentally measured spectrum and the composition of primary cosmic rays (CR) in the energy range comprising the knee: 1) the model by

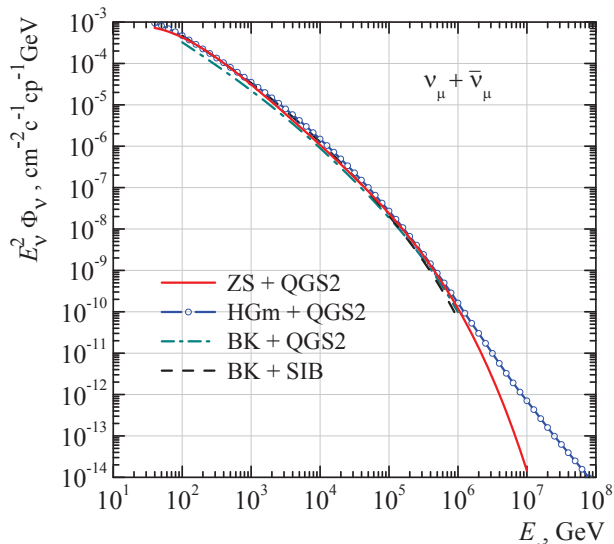


FIG. 1. Comparison $\nu_\mu + \bar{\nu}_\mu$ fluxes calculated for 3 PCR models.

Zatsepin & Sokolskaya [17], 2) the modified multi-knee model by Bindig, Bleve and Kampert [18], and 3) the novel model of primary spectrum by Gaisser [19], based on assumption that there are three classes of CR sources: i) Galactic supernova remnants, ii) Galactic high-energy sources different from the former, iii) extragalactic astrophysical objects (mixed composition).

II. FLUXES OF ATMOSPHERIC MUON NEUTRINOS

The calculation is performed on the basis of the method [20] of solution of the hadronic cascade equations in the atmosphere, which allows to describe the hadron-nucleus cascade induced by cosmic rays in air taking into the nonpower law energy spectrum of the primary cosmic rays, the violation of Feynman scaling, and the growth of the total inelastic cross sections for hadron-nucleus collisions with increasing energy (see also [14]). Along with major sources of the muon neutrinos, $\pi_{\mu 2}$ and $K_{\mu 2}$ decays, we consider three-particle semileptonic decays, $K_{\mu 3}^\pm$ (the branching ratio 3.32%), $K_{\mu 3}^0$ (27%), the contribution originated from decay chains $K \rightarrow \pi \rightarrow \nu_\mu$ ($K_S^0 \rightarrow \pi^+\pi^-$, $K^\pm \rightarrow \pi^\pm\pi^0$), as well as small fraction from the muon decays. The sources of the conventional ν_e are three-particle decays of kaons K_{e3}^\pm , K_{e3}^0 with the branching ratio 5.07% and 40.5% respectively. The latter is dominant source of electron neutrinos at energy below 10 TeV. μ_{e3} decays also contribute.

As the primary cosmic ray spectra and composition in wide energy range we use in our calculations following models: 1) the model by Zatsepin & Sokolskaya (ZS), 2) the modified multi-knee model by Bindig, Bleve and Kampert (BK) [18] based on KASCADE data [21] and the polygonato model by Hörandel [22], and 3) the novel

CR approximation by Hillas-Gaisser [19], a version for the mixed CR population 3 (denoted here as HGm that corresponds to the H3a of Ref.[23]) which takes into consideration also the measurement data by HiRes, PAO and Telescope Array.

The model by Zatsepin and Sokolskaya [17] describes well data of the ATIC2 direct measurements [24] in the range $10 - 10^5$ GeV and gives a motivated extrapolation of these data up to 100 PeV – the energy region, for which the cosmic ray spectrum and composition is derived from measured characteristics of EAS. The ZS proton spectrum at $E \gtrsim 10^6$ GeV is compatible with KASCADE data as well the helium one within the range of the KASCADE spectrum obtained with the usage of hadronic models QGSJET01 and SIBYLL, and well agree with the HGm up to 1 PeV. Comparison of the muon neutrino fluxes calculated with three recent primary spectrum model models (Fig. 1) shows that they are rather close each other up to 1 PeV.

In Table I presented are neutrino flux ratios (averaged over zenith angles) calculated with usage of three hadronic models QGSJET-II, SIBYLL and KM: columns marked as 1, 2, 3 present comparative ($\nu_\mu + \bar{\nu}_\mu$) fluxes, $\phi_{\nu_\mu}^{(\text{SIBYLL})}/\phi_{\nu_\mu}^{(\text{QGSJET II})}$, $\phi_{\nu_\mu}^{(\text{KM})}/\phi_{\nu_\mu}^{(\text{QGSJET II})}$, and $\phi_{\nu_\mu}^{(\text{SIBYLL})}/\phi_{\nu_\mu}^{(\text{KM})}$ respectively. Columns 4, 5, 6 give the same for the ($\nu_e + \bar{\nu}_e$) flux. All computations are performed for ZS and HGm cosmic ray spectra. One can see that QGSJET II and SIBYLL 2.1 lead to apparent difference in the muon neutrino flux, as well as in the case of SIBYLL as compared to KM. The origin of differences is evident: the hadronic models bear the imprint of the kaon production ambiguity.

In Figs. 2, 3, the conventional and prompt ($\nu_\mu + \bar{\nu}_\mu$) flux averaged over zenith angles in the range $0^\circ - 83^\circ$ (corresponding to $97^\circ - 180^\circ$ for the upward neutrinos) calculated with use of ZS and BK spectra are compared

TABLE I. Relative ν_μ and ν_e fluxes calculated with SIBYLL 2.1, QGSJET II-03 and KM hadronic models for ZS [17] and HGm [19] cosmic ray spectra: 1 (4) – sib/qgs2; 2 (5) – km/qgs2; 3 (6) – sib/km.

E_ν , GeV	1	2	3	4	5	6
	ZS: ($\nu_\mu + \bar{\nu}_\mu$)			ZS: ($\nu_e + \bar{\nu}_e$)		
10^3	1.70	1.05	1.62	1.41	0.51	2.76
10^4	1.53	1.04	1.47	1.32	0.48	2.75
10^5	1.53	1.10	1.39	1.29	0.54	2.39
10^6	1.79	1.64	1.09	1.41	0.84	1.68
10^7	1.85	2.08	0.89	1.38	1.06	1.30
	HGm: ($\nu_\mu + \bar{\nu}_\mu$)			HGm: ($\nu_e + \bar{\nu}_e$)		
10^3	1.59	0.85	1.87	1.39	0.49	2.84
10^4	1.57	1.12	1.40	1.33	0.50	2.66
10^5	1.57	1.27	1.24	1.31	0.57	2.30
10^6	1.63	1.63	1.00	1.31	0.70	1.87
10^7	1.47	1.53	0.96	1.23	0.59	2.08

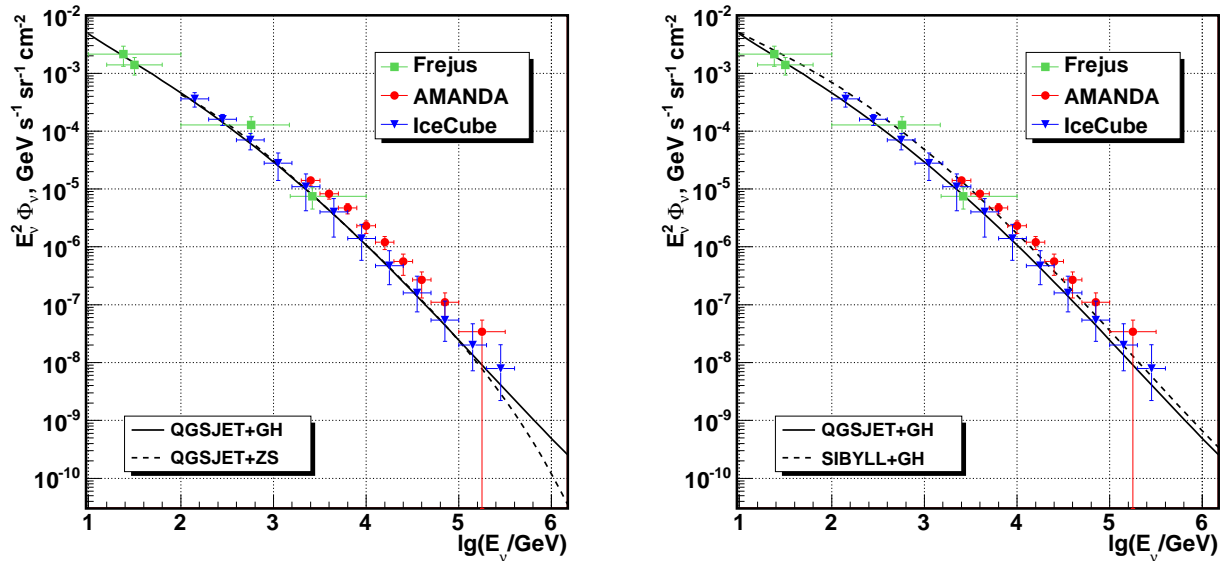


FIG. 2. Conventional ($\nu_\mu + \bar{\nu}_\mu$) spectrum averaged over zenith angles: a dependence on the cosmic ray spectrum (left panel) and the hadronic model (right). Symbols: data of Frejus [7], AMANDA-II [8] and IceCube [2] experiments.

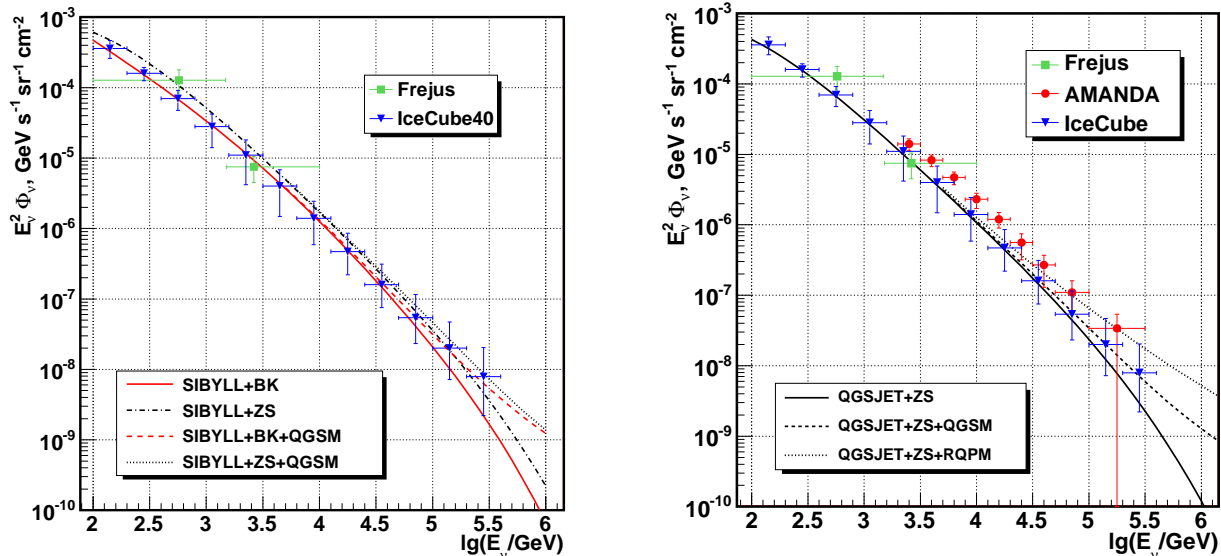


FIG. 3. Fluxes of the conventional and prompt (QGSM, RQPM) muon neutrinos ($\nu_\mu + \bar{\nu}_\mu$) calculated with usage of SIBYLL 2.1 (left panel) and QGSJET II (right panel) for the cosmic ray spectra with the knee.

with Frejus [7] (squares), AMANDA-II [8] (circles), and IceCube [2] (triangles) measurement data. To illustrate the influence of the “knee” in cosmic ray spectrum, in Fig. 2 we plotted also the conventional ($\nu_\mu + \bar{\nu}_\mu$) spectrum computed with usage of the CR parametrization by Gaisser, Honda, Lipari and Stanev (GH) [25]. The right panel of Fig. 2 shows an influence of the hadronic models, QGSJET vs. SIBYLL (see also Tabl. I). The difference in the neutrino flux predictions resulted from

CR spectra becomes apparent at high neutrino energies: the flux obtained with QGSJET II-03 for GH spectrum at 600 TeV is nearly twice as large as that for ZS spectrum. Close to 1 PeV this discrepancy increases to the factor five. More results concerning the muon neutrino calculations compared to the AMANDA and IceCube40 measurements were presented in Refs. [26–28].

The prompt neutrino flux was calculated using the quark-gluon string model (QGSM) by Kaidalov

& Piskunova [30, 31] as well as the recombination quark-parton model (RQPM) [31]. In Fig. 3 the prompt neutrino calculations were performed with the old parametrization of cosmic ray spectrum by Nikolsky, Stamenov and Ushev (NSU) [32], therefore they can serve here as upper limits for the prompt neutrino flux due to RQPM or QGSM. Addition of the QGSM prompt contribution improves the agreement with the Icecube measurement data above 100 TeV. Note the prompt neutrino flux obtained with the dipole model (DM) [33] is in close agreement to the QGSM prediction [31] above 1 PeV. The prompt neutrino flux due to QGSM or RQPM can be approximated at energies $5 \text{ TeV} \leq E \leq 5 \text{ PeV}$ by the expressions

$$\phi_{\nu}^{(\text{qgsm})}(E) = A(E/E_1)^{-3.01}[1+(E/E_1)^{-2.01}]^{-0.165}, \quad (1)$$

$$\phi_{\nu}^{(\text{rqpm})}(E) = B(E/E_1)^{-2.96}[1+(E/E_1)^{-1.96}]^{-0.157}, \quad (2)$$

where $A = 1.19 \cdot 10^{-18}$, $B = 4.65 \cdot 10^{-18} (\text{GeV cm}^2 \text{ sr})^{-1}$, $E_1 = 100 \text{ TeV}$.

The muon neutrino flux calculations both for ZS cosmic ray spectrum and HGm one in comparison with recent ANTARES measurement data [5] along with IceCube data [2] are presented in Fig. 4. The conventional flux due to the (HGm + QGSJET II) example (black solid line) is similar to that of ZS+QGSJET II (blue dashed line) up to 1 PeV. The QGSM prompt muon flux is displayed in Fig. 4 in two ways: green dots mark result obtained with NSU spectrum and red solid line shows the sum of conventional flux (ZS + QGSJET II) and the prompt one obtained by rescaling of NSU result to the ZS cosmic ray spectrum.

We can describe the conventional ($\nu_{\mu} + \bar{\nu}_{\mu}$) flux (HGm + QGSJET II example) as well as ($\nu_e + \bar{\nu}_e$) one by the approximation valid for $10^2 - 10^7 \text{ GeV}$ with errors not exceed 12% (at lower energies) (in units of $\text{cm}^{-2}\text{s}^{-1}\text{sr}^{-1}\text{GeV}^{-1}$):

$$\lg[E_{\nu}^2 \phi_{\nu_{\mu}}^{\pi, K}(E_{\nu})] = -(2.31 + 0.198y + 0.165y^2 + 0.00146y^3), \quad (3)$$

$$\lg[E_{\nu}^2 \phi_{\nu_e}^{\pi, K}(E_{\nu})] = -(2.26 + 0.791y + 0.0743y^2 + 0.00548y^3), \quad (4)$$

where $y = \lg(E_{\nu}/\text{GeV})$. Fluxes of neutrinos can be also written in the form:

$$\phi_{\nu}^{\pi, K}(E_{\nu}) = C_{\nu} \left(\frac{E_{\nu}}{1 \text{ GeV}} \right)^{-(\gamma_0 + \gamma_1 y + \gamma_2 y^2)}. \quad (5)$$

Two sets of the parameters to Eq. (5) are given in Table II for the conventional spectra ($\nu_{\mu} + \bar{\nu}_{\mu}$) and ($\nu_e + \bar{\nu}_e$).

The difference of muon neutrino flux predictions originated from the primary cosmic ray spectra, including the knee, becomes apparent above 1 PeV: the flux obtained with QGSJET II for ZS spectrum at 2 PeV is less by a third of the flux for HGm spectrum. Better angular resolution in ANTARES experiment ($< 1^{\circ}$) [5] as compared

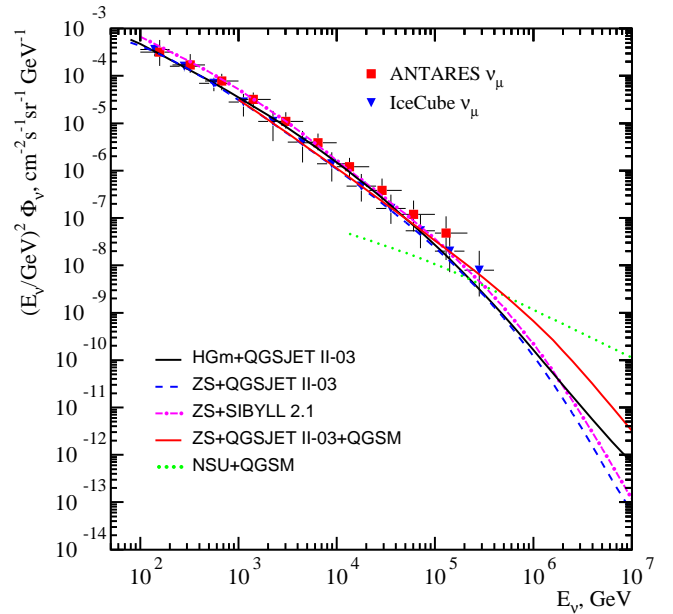


FIG. 4. The conventional and prompt (QGSM) ($\nu_{\mu} + \bar{\nu}_{\mu}$) flux against the ANTARES and IceCube measurement data.

with that of Icecube ($> 10^{\circ}$) for shower-like events [10]) leads probably to events abundance close to horizontal directions. The lower limit (-0.12) of the integral over cosine of zenithal angle which corresponds to $\theta > 97^{\circ}$ in IceCube experiment [2] implies the neutrino flux to be less by (15 – 25)% (in the energy range 1 – 100 TeV) as compared to that in ANTARES with $\theta > 90^{\circ}$ condition [5]. Besides the large angle errors near vertical direction can be transformed to considerable distortion of the neutrino energy spectrum due to neutrino absorption in the Earth depending on zenith angle. Note that ANTARES’s procedure to calculate the neutrino absorption differs from that of IceCube.

Calculated atmospheric muon neutrino fluxes for the energy range 0.4 – 1 PeV are presented also in Table III along with upper limits on the astrophysical muon neutrino diffuse flux obtained with the ANTARES [6] and IceCube59 [23]. The total atmospheric muon neutrino flux (sum of the conventional flux and prompt one) marked in Table III as “conv. (averaged)+ QGSM/DM” is presented by the calculation sample HGm+QGSJET II + QGSM/DM. More intent inspection of the predicted atmospheric neutrino fluxes (Table III), both conventional and prompt, shows that distinctions between the

TABLE II. Parameters for the conventional neutrino spectra (see Eq. (5)).

flavor	C_{ν}	γ_0	γ_1	γ_2
$\nu_{\mu} + \bar{\nu}_{\mu}$	$4.896 \cdot 10^{-3}$	2.198	$1.648 \cdot 10^{-1}$	$1.46 \cdot 10^{-3}$
$\nu_e + \bar{\nu}_e$	$5.466 \cdot 10^{-3}$	2.791	$7.427 \cdot 10^{-2}$	$5.48 \cdot 10^{-3}$

TABLE III. Atmospheric neutrino flux at $E_\nu = 1$ PeV and upper limit for diffuse ($\nu_\mu + \bar{\nu}_\mu$) flux obtained with neutrino telescopes.

Model	$E_\nu^2 \phi_\nu$, GeV (cm ² sr) ⁻¹
conventional $\nu_\mu + \bar{\nu}_\mu$: averaged over angles –	400 TeV - 1 PeV
ZS [17]+SIBYLL 2.1	$(2.21 - 0.214) \times 10^{-9}$
ZS+QGSJET II	$(1.32 - 0.149) \times 10^{-9}$
BK [18]+QGSJET II	$(1.09 - 0.097) \times 10^{-9}$
HGm [19]+QGSJET II	$(1.45 - 0.163) \times 10^{-9}$
selected zenith angles:	$E_\nu = 1$ PeV
HGm+QGSJET II, $\cos \theta = 0.5$	1.09×10^{-10}
HGm+QGSJET II, $\cos \theta = 0.3$	1.76×10^{-10}
HGm+QGSJET II, $\cos \theta = 0.1$	3.84×10^{-10}
prompt $\nu_\mu + \bar{\nu}_\mu$:	400 TeV - 1 PeV
NSU [32]+QGSM [31]	$(2.86 - 1.15) \times 10^{-9}$
HGm+QGSM	$(2.2 - 0.54) \times 10^{-9}$
$174E_N^{-3} + \text{DM}$ [33]	$(1.87 - 0.85) \times 10^{-9}$
conv. + prompt $\nu_\mu + \bar{\nu}_\mu$:	$E_\nu = 1$ PeV
conv.(averaged)+ QGSM	0.70×10^{-9}
conv.(averaged)+ DM	1.01×10^{-9}
conv. ($\cos \theta = 0.1$)+QGSM	0.92×10^{-9}
diffuse $\nu_\mu + \bar{\nu}_\mu$:	
IC59 best fit	2.5×10^{-9}
IC59 limit [23]	1.44×10^{-8}
(34.5 TeV - 36.6 PeV)	
ANTARES limit [6]	4.8×10^{-8}
(45 TeV - 10 PeV)	

DM and QGSM prompt muon neutrino flux predictions are hardly observable at the present level of the experimental errors, if the knee of the cosmic ray spectrum is taken into account.

III. ELECTRON NEUTRINO FLUX AND THE NEUTRINO FLAVOR RATIO

Recently the IceCube published results for the electron neutrino spectrum measured in the energy range ~ 80 GeV - 6 TeV [9], making possible evaluation the neutrino flavor ratio and comparison it with predictions. Results of calculation of the atmospheric ($\nu_e + \bar{\nu}_e$) flux with QGSJET II-03 and SIBYLL 2.1 for three parametrizations of cosmic ray spectra are presented in Fig. 5 along the measurement data. In Fig. 5 is shown also (right panel) the contribution of diffuse flux (red dashed and dash-dotted lines) of cosmic neutrinos added to the atmospheric conventional neutrino flux which are calculated with usage of QGSJET II-03 for the Hillas-Gaisser spectrum (HGm). Upper dashed red line in this figure depicts the the sum of the atmospheric electron neutrino flux and the diffuse flux of cosmic neutrinos with an the E^{-2} -

spectrum, $E_\nu^2 \phi_\nu = 3.6 \cdot 10^{-8}$, (cm² s sr)⁻¹ GeV (assuming a flavor ratio of $\nu_e : \nu_\mu : \mu_\tau = 1 : 0 : 0$). The dash-dotted red line corresponds to sum of atmospheric electron neutrinos and astrophysical ones, $E_\nu^2 \phi_\nu = 1.2 \cdot 10^{-8}$, (cm² s sr)⁻¹ GeV, for the assumption $\nu_e : \nu_\mu : \mu_\tau = 1 : 1 : 1$. This limit obtained by IceCube [4] for the energy range above 1 PeV is compatible with the two PeV neutrino events [11] with energies 1.04 ± 0.16 and 1.14 ± 0.17 PeV which were detected by the IceCube neutrino telescope.

Since IceCube has measured energy spectra both of muon and electron neutrino, we can try to construct the neutrino flavor ratio $R_{\nu_\mu/\nu_e} = \phi_{\nu_\mu + \bar{\nu}_\mu} / \phi_{\nu_e + \bar{\nu}_e}$ and check for agreement the calculations with experimental data. The conventional neutrino flavor ratio, R_{ν_μ/ν_e} , calculated for different parametrizations of cosmic ray spectra, as it is seen in Fig. 6, is rather sensitive to hadronic models than to the primary spectrum. The difference of neutrino flux predictions related to choice of hadronic models is clearly seen: curves display the scale of difference between the conventional ($\nu_\mu + \bar{\nu}_\mu$) and ($\nu_e + \bar{\nu}_e$) spectra, calculated with usage of QGSJET II, SIBYLL for three parametrizations of cosmic-ray spectra, HGm, ZS and BK.

The dotted line (HKKM, 2007) in Fig. 6 (left panel) is for the Monte Carlo calculation by Honda et al. [35] made with usage of the hadronic model DPMJET-III [36, 37] (here we draw result for $\cos \theta = 0.2 - 0.3$, which approaches the average ratio). The top curve (the line with open circles) shows R_{ν_μ/ν_e} calculated with the KM hadronic model. Definitely this figure displays significant discrepancy between DPMJET-III and KM on the one hand, QGSJET II and SIBYLL on the other, which is entirely attributable to the difference of hadronic models in kaon yield in nuclon-nuclei collisions. However the dissimilarity in R_{ν_μ/ν_e} between SIBYLL and QGSJET II is not so large as one might expect from the difference of kaon yield.

The thick green dashed line in Fig. 6 (right panel) corresponds to a reconstruction of the ratio R_{ν_μ/ν_e} based on both muon and electron neutrino spectra measured in IceCube experiment [2, 9]. The electron neutrino spectrum above 5 TeV we extrapolated up to 10 TeV. The fill area in Fig. 6 reflects a rough estimate of the IceCube data uncertainties, thick dash line is median one. Curves marked as 1 and 2 in Fig. 6 depict the total neutrino flavor ratio comprising the conventional, prompt and astrophysical neutrinos. The latter were added in line with with two assumptions indicated in Fig 5 (right panel). Thus one may assume that IceCube atmospheric neutrino measurement data give an indication that astrophysical electron neutrinos probably contribute to the flux in the energy region above 10 TeV.

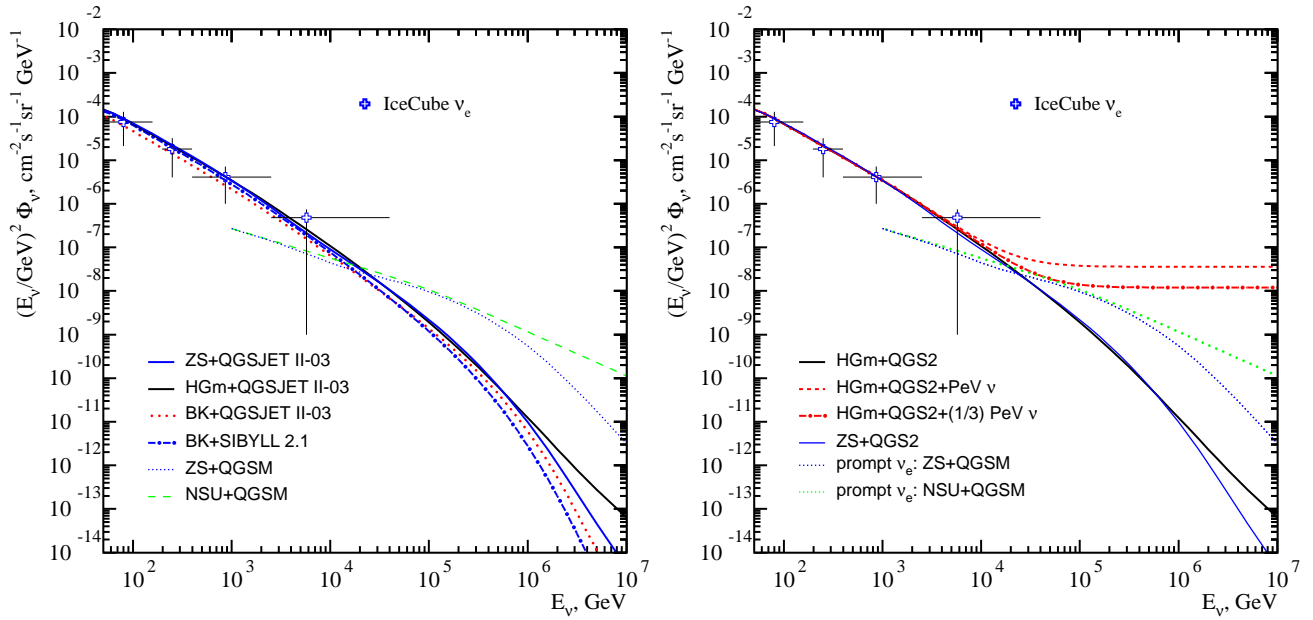


FIG. 5. Atmospheric ($\nu_e + \bar{\nu}_e$) spectrum and the diffuse flux of cosmic neutrinos (see text for explanation).

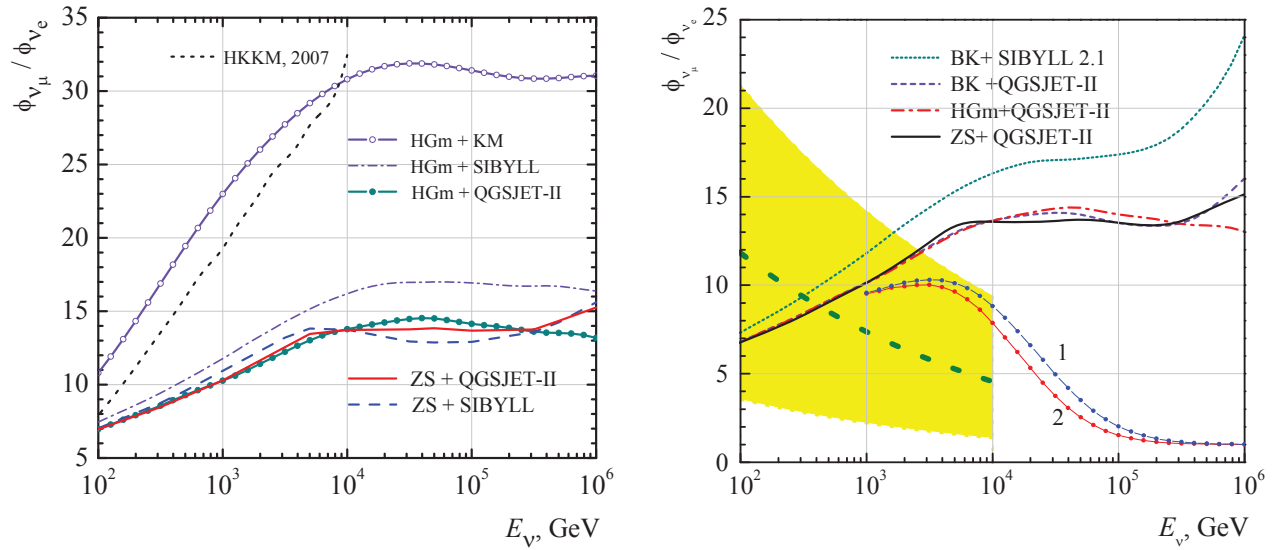


FIG. 6. The neutrino flavor ratio R_{ν_μ/ν_e} . Left panel: Conventional neutrino flavor ratio depending on the hadronic model and cosmic ray spectrum. The lines show the angle-averaged ratio calculated for the cosmic-ray spectra HGm [19] and ZS [17] but the dotted line (HKKM, 2007), which presents the calculation by Honda et al. [35] for $\cos\theta = 0.2 - 0.3$. Right panel: A reconstruction of R_{ν_μ/ν_e} based on the neutrino spectra measured by IceCube [2, 9] in comparison with results obtained for BK [18], HGm and ZS primary spectra. The yellow band images an estimate of the IceCube data uncertainties, thick dashed line is median one. Lines 1, 2 show the total R_{ν_μ/ν_e} comprising the conventional, prompt and diffuse neutrinos.

IV. DISCUSSION AND SUMMARY

The calculation of the high-energy atmospheric neutrino flux demonstrates rather weak dependence on the cosmic ray spectrum in the energy range $10^2 - 10^5$ GeV. However the picture appears to be less steady because of sizable flux differences resulting from models of high-energy hadronic interactions. As it can be seen by the

example of the models QGSJET II-03 and SIBYLL 2.1, the major factor of the discrepancy in conventional neutrino fluxes is the kaon production in nucleon-nucleus collisions. Really, cosmic-ray physicists feel necessity of comprehensive analysis of the actual features of the high-energy hadronic models under discussion, QGSJET II-03 (04), EPOS-LHC, SIBYLL 2.1, DPMJET-III, especially concerning details of charged and neutral kaon produc-

tion in NA - and πA -collisions.

To illustrate in part the difference of the hadronic models one can compute the cosmic ray spectrum-weighted moments (z -factors) for proton-air interactions $pA \rightarrow cX$ of the inclusive spectra $(x/\sigma_{pA}^{in})(d\sigma_{pc}/dx)$:

$$z_{pc}(E_0) = \int_0^1 \frac{x^\gamma}{\sigma_{pA}^{in}} \frac{d\sigma_{pc}}{dx} dx, \quad (6)$$

where $x = E_c/E_0$, $\gamma = 1.7$, $c = \pi^\pm, K^\pm$. z -factors for DPMJET-III are taken from Ref. [37] (see [36]). As one can see in Table IV, z -factors demonstrate approximate scaling law in DPMJET-III, KM and SIBYLL 2.1 (but the production of K -mesons) while in case of QGSJET-II a noticeable violation of the scaling is found just for pions.

TABLE IV. z_{pc} -factors for π and K mesons.

Model	E_0 ,	$z_{p\pi^+}$	$z_{p\pi^-}$	z_{pK^+}	z_{pK^-}
QGSJET	10^2	0.043	0.035	0.0036	0.0030
	10^3	0.036	0.029	0.0036	0.0028
	10^4	0.033	0.028	0.0034	0.0027
SIBYLL	10^2	0.036	0.026	0.0134	0.0014
	10^3	0.038	0.029	0.0120	0.0022
	10^4	0.037	0.029	0.0097	0.0026
KM	10^2	0.044	0.027	0.0051	0.0015
	10^3	0.046	0.028	0.0052	0.0015
	10^4	0.046	0.029	0.0052	0.0015
DPMJET	10^3	0.04	0.035	0.0070	0.0035
	10^4	0.04	0.035	0.0070	0.0031

Note that relative proximity of z -factors for KM and DPMJET-II models leads to similar behaviour of the neutrino flavor ratio, R_{ν_μ/ν_e} (left panel of Fig. 6). Relative kaon excess due to KM, DPMJET-III and SIBYLL makes some kind “hierarchy” of the plateau in the energy dependence of R_{ν_μ/ν_e} (still corrected for different pion yield):

$$R_{\nu_\mu/\nu_e}^{(QGSJET)} < R_{\nu_\mu/\nu_e}^{(SIBYLL)} < R_{\nu_\mu/\nu_e}^{(DPMJET)} < R_{\nu_\mu/\nu_e}^{(KM)}.$$

Bearing in mind the sizable difference of the kaon yield in SYBYLL 2.1, QGSJET-II and DPMJET-III, the closeness of R_{ν_μ/ν_e} in the MC calculations (using the code CORSIKA) [34] for SIBYLL and QGSJET-II models is not so evident. The MC computation gives larger value of R_{ν_μ/ν_e} , up to 25 – 30 (see Fig. 2 in Ref. [34]), as compared to that of present work, 14 – 17. In particular, R_{ν_μ/ν_e} above 1 TeV obtained in Ref. [35] as well as R_{ν_μ/ν_e} in our calculation for the KM hadronic model, is hardly compatible with the neutrino flavor ratio reconstructed from IceCube data (Fig. 6): $R_{\nu_\mu/\nu_e}^{(HKKM)} \approx 10, 20, 30$ for $E_\nu = 0.1, 1, 10$ TeV respectively. The computation [35] performed with use of DPMJET-III [36, 37] gives rather

low ν_e flux (due to less abundance of K -mesons) as compared to that for case of SIBYLL (factor about 3) or even for QGSJET-II (factor near 2) while ν_μ fluxes are rather close each other. This factor leads to large difference in R_{ν_μ/ν_e} . The hadronic model by Kimel and Mokhov leads to the neutrino flavor ratio, R_{ν_μ/ν_e} , very close to result for DPMJET-III at least in the energy range 100 GeV – 10 TeV, but there are important details concerned the kaons.

Above 100 TeV calculated spectra of muon neutrinos display apparent dependence on the spectrum model and composition of primary cosmic rays related to the “knee”. Also in this region uncertainties appear due to production cross sections and decays of charmed particles which imprint on the prompt neutrino flux. The total flux of the conventional and prompt neutrinos calculated with QGSJET II-03 and QGSM describes the IceCube data well enough. The QGSM predicted muon neutrino flux in the range 0.4 – 1 PeV one does not violate the upper limit on the diffuse flux of astrophysical neutrinos obtained by IceCube59 [23].

The diffuse flux of astrophysical neutrinos related to the PeV neutrino events in the IceCube experiment should lead to a decrease of the neutrino flavor ratio R_{ν_μ/ν_e} , at the energy above 10 TeV. An extrapolation of the IceCube diffuse PeV neutrino flux to the energy range below 30 TeV shows the consistency of calculated R_{ν_μ/ν_e} and that of obtained from the IceCube data. The computation hints that confirmation of astrophysical origin for high-energy neutrino events might be obtained from little progress in measurement of ν_e spectrum above 10 TeV, since R_{ν_μ/ν_e} , more sensitive to the electron neutrino flux, allows to reveal a small fraction from astrophysical sources.

Observation of the PeV-energy neutrino events by IceCube [11] changes drastically the situation concerning the prompt neutrino contribution. If the first indication of astrophysical neutrinos by IceCube would be confirmed in further studies (particularly in the measurement of electron neutrino flux above 10 TeV), then the atmospheric ν_e flux uncertainty due to the charm production becomes unimportant at the energy above 10 TeV (see Fig. 5).

Neutrino flavor ratio extracted from IceCube data does not reveal a trend to rise as it would be expected for the conventional neutrino flux (Fig. 6). An explanation of this apparent tendency can be related to diffuse neutrinos appeared against background of the atmospheric electron neutrino flux because latter is lower as compared to muon neutrinos. Preliminary and superficial analysis leads to the assumption: IceCube atmospheric neutrino data give indication that astrophysical electron neutrinos should be observable at the energy some 10 TeV, if the power law E^{-2} is valid for astrophysical neutrino spectrum in this range. Whether this optimism has any grounding in reality remains to be seen.

ACKNOWLEDGMENTS

This work is supported by the Ministry of Education and Science of Russian Federation (Zadanie 3.889.2014/k).

-
- [1] V. Aynutdinov et al., Nucl. Instrum. Meth. A **588**, 99 (2008).
- [2] R. Abbasi et al. (IceCube Collaboration), Phys. Rev. D **83**, 012001 (2011).
- [3] R. Abbasi et al. (IceCube Collaboration), Phys. Rev. D **84** (2011) 082001.
- [4] R. Abbasi et al. (IceCube Collaboration), Phys. Rev. D **83**, 092003 (2011).
- [5] S. Adrian-Martinez et al. Eur. Phys. J. C **73**, 2606 (2013).
- [6] V. Van Elewyck (ANTARES Collaboration), Nucl. Instrum. Meth. A **742**, 63 (2014).
- [7] K. Daum et al., Z. Phys. C **66**, 417 (1995).
- [8] R. Abbasi et al. (IceCube Collaboration), Astropart. Phys. **34**, 48 (2010).
- [9] M. G. Aarsten et al. (IceCube Collaboration), Phys. Rev. Lett. **110**, 151105 (2013).
- [10] M. G. Aartsen et al. (IceCube Collaboration), Science **342**, 1242856 (2013).
- [11] M. G. Aartsen et al. (IceCube Collaboration), Phys. Rev. Lett. **111**, 021103 (2013).
- [12] S. Ostapchenko, Phys. Rev. D **74**, 014026 (2006); Nucl. Phys. B (Proc. Suppl.) **175-176**, 73 (2008).
- [13] E.-J. Ahn et al. Phys. Rev. D **80**, 094003 (2009).
- [14] A.A. Kochanov, T.S. Sinogovskaya, S.I. Sinogovsky, Astropart. Phys. **30**, 219 (2008).
- [15] A.A. Kochanov, T.S. Sinogovskaya, S.I. Sinogovsky, J. Exp. Theor. Phys. **116**, 395 (2013); Zh. Eksp. Teor. Fiz. **143**, 459 (2013).
- [16] A.N. Kalinovsky, N.V. Mokhov, Yu.P. Nikitin, 1989. Passage of high-energy particles through matter, New York, USA: AIP (1989) 262 p.
- [17] V.I. Zatsepin, N.V. Sokolskaya, Astronomy & Astrophys. **458**, 1 (2006).
- [18] D. Bindig, C. Bleve, K.-H. Kampert, in Proc. of 32nd ICRC, Beijing, 2011, Vol. 1, p. 161.
- [19] T. K. Gaisser, Astropart. Phys. **35**, 801 (2012); T. Gaisser, arXiv:1303.1431.
- [20] V. A. Naumov, T. S. Sinogovskaya, Phys. Atom. Nucl. **63**, 1927 (2000); hep-ph/0106015.
- [21] T. Antoni et al., Astropart. Phys. **24**, 1 (2005).
- [22] J. Horandel, Astropart. Phys. **21**, 241 (2004).
- [23] M. G. Aarsten et al. (IceCube Collaboration), arXiv:1311.7048.
- [24] A. D. Panov et al., Bull. Russ. Acad. Sci. Phys. **71**, 494 (2007); *ibid.* **73**, 564 (2009)
- [25] T.K. Gaisser, M. Honda, Annu. Rev. Nucl. Part. Sci. **52**, 153 (2002).
- [26] S. I. Sinogovsky, O.N. Petrova, T. S. Sinogovskaya, in Proc. of 32nd ICRC, Beijing, 2011, Vol. 4, p. 291; arXiv:1109.3576.
- [27] O. N. Petrova, T. S. Sinogovskaya, S. I. Sinogovsky, Phys. Part. Nucl. Lett. **9**, 766 (2012).
- [28] S. I. Sinogovsky, E. V. Ogorodnikova, T. S. Sinogovskaya, arXiv:1306.5907v2.
- [29] T.K. Gaisser, M. Honda, Annu. Rev. Nucl. Part. Sci. **52**, 153 (2002).
- [30] A. B. Kaidalov, O. I. Piskunova, Sov. J. Nucl. Phys. **41**, 816 (1985); Sov. J. Nucl. Phys. **43**, 994 (1986); Z. Phys. C **30**, 145 (1986).
- [31] E.V. Bugaev et al. Nuovo Cim. C **12**, 41 (1989).
- [32] S.I. Nikolsky, I.N. Stamenov, S.Z. Ushev, Zh. Eksp. Teor. Fiz. **87**, 18 (1984) [Sov. Phys. JETP **60**, 10 (1984)].
- [33] R. Enberg, M.H. Reno, I. Sarcevic, Phys. Rev. D **78**, 043005 (2008).
- [34] A. Fedynitch, J. Becker Tjus, P. Desiati, Phys. Rev. D **86**, 114024 (2012).
- [35] M. Honda et al., Phys. Rev. D **75**, 043006 (2007).
- [36] S.Rostler, R.Engel, J. Ranft, hep-ph/0012252.
- [37] T.Sanuki et al., Phys. Rev. D **75**, 043005 (2007).